scientific reports

Check for updates

OPEN

Digitalised phenotyping of pepper (*Capsicum* spp.) using effective RGB imaging and optimised camera positioning

Eric Opoku Mensah[1,3,6], Jiseon Song[1], Hyeonseok Oh[2], Alebel Mekuriaw Abebe[1], Yong Suk Chung[4], Jeongho Baek[1,6]✉ & Sheikh Mansoor[5]✉

Recent technological advancements employ imaging techniques to examine the morphological, physiological, and genetic differences among plant accessions, enhancing precision and productivity. High-throughput phenotyping serves as an essential method for selecting traits and reducing errors tied to manual data collection. However, the effects of camera-to-object distance in imaging acquisition for plant phenomics have received less attention. We analyzed the imaging parameters that define well the morphological characteristics of pepper and the effects of camera-to-object distance on the imaging of plant growth, leaf dimensions, fruit, and seed characteristics. Three camera-to-object distances (0.8, 1.0, and 1.2 m) were studied for the vegetative stage, and six camera-to-object distances (0.35–0.85 m) were used for the reproductive stages. The results demonstrated that imaging parameters such as *Major* (the longest line that can be drawn within the leaf) and *Minor* (the shortest line perpendicular to the major axis) are more effective for assessing canopy spread, while imaging *Height* provides a strong correlation ($r = 0.9$) for actual plant height measurement. An optimal camera-to-object distance of 0.8 m yielded better correlations for vegetative traits across all pepper genotypes, likely due to resolution factors at different growth stages. For fruit and seed traits, shorter distances of 0.55 m and 0.65 m were suitable. Additionally, the weights of fresh and dry fruit correlated highly with image area ($r = 0.94$ and 0.89, respectively, at 0.55 m). The studied pepper genotypes exhibited distinct seed characteristics, including variations in *Roundness*, *Solidity*, and *Circularity*. The imaging approach can accurately capture various plant characteristics and has the potential to replace traditional methods for assessing plants.

Keywords Pepper, Imaging, RGB, Plant growth, Leaf dimensions, Fruit, Seed characteristics

Pepper *(Capsicum* spp.), one of the *Solanaceae* family, is diverse, including domesticated, semi-domesticated, and wild relatives[1]. The diversity comprises diploid genotypes with 12-chromosome number ($2n = 2x = 24$), 13 chromosome number ($2n = 2x = 26$), and tetraploid species ($2n = 4x = 48$), a wild form of the cultivated species[2]. About 31 species of the genus are documented, including 26 wild and 5 cultivated[3]. The cultivated species include *C. annuum* L., *C. frutescens* L., *C. chinense* Jacq., *C. baccatum* L., and *C. pubescens* Ruiz & Pav., along with other related complex genotypes, which arise from varying levels of cross-pollination among the species[4–6].

Pepper domestication and selection have enhanced yield and resistance to biotic and abiotic stress factors over the years[7]. Traits such as vegetative (including growth habit, leaf architecture, and canopy spread) and fruit characteristics (fruit shape, size, color, pungency, seeds per fruit, and wall thickness) have been used for selection for breeding or production[2]. Trait selections have, over the years, been through visual assessments, conventional breeding programs, or, in a detailed method, at the DNA level using molecular markers[8–10]. However, the lack of efficient methods to identify and quantify some specific traits, such as growth and yield-related traits, is one of

[1]Gene Engineering Division, National Institute of Agricultural Sciences, Rural Development Administration, Jeonju 54874, Republic of Korea. [2]National Agrobiodiversity Center, National Institute of Agricultural Sciences, Rural Development Administration, Jeonju 54874, Republic of Korea. [3]CSIR – Plant Genetic Resources Research Institute (CSIR-PGRRI), P. O. Box 7, Bunso, Eastern Region, Ghana. [4]Department of Plant Resources and Environment, Jeju National University, Jeju 63243, Republic of Korea. [5]Department of Horticulture, Faculty of Agriculture, Recep Tayyip Erdoğan University, Rize/Pazar, Türkiye 53300, Turkey. [6]Eric Opoku Mensah and Jeongho Baek contributed equally to this work. ✉email: firstleon@korea.kr; mansoorshafi21@gmail.com

the major gaps in pepper breeding[3,11]. The gaps are associated with challenges involving climate change-related scenarios, pests and disease, the demands and preferences of consumers, and food security[12]. Nevertheless, pepper production continues to support many households, especially in Africa and Asia[13,14]. To ensure the sustainability and biological diversity of pepper, new and modern breeding programs are important to meet climate-related challenges and consumer demands.

Pepper imaging can be a way out[11,15–17]. The technique, known as high-throughput phenotyping, plays an important role in trait selection and reduces errors in manual measurements[18,19]. Imaging is non-destructive and combines a high-throughput algorithm software to detect individual plant parts for analysis[20,21]. For example, the imaging approach has been used to study the performances of modelled plants such as *Arabidopsis*, *Oryza*, *and Triticum*[17,18,22], plant diseases[23], or to identify the water and temperature relations between some crops and their environment[16,24] and diversity among some vegetables[20,25]. In view, different imaging software such as ImageJ for whole plant analysis, Tomato Analyzer for tomato image analysis, LeafAnalser and LAMINA for leaf shapes, and SmartGrain for seed analysis, are developed to enhance automated phenotyping of plants[26–30].

Though efforts are made[31,32], pepper imaging is at the basic stage[3,11], as some challenges, such as plant architecture and overlapping of fruits and flowers, are yet to be solved[33]. Again, challenges with the imaging of some fruit traits, such as size, shape, surface appearance, and color, are not fully solved. Over the years, a group of researchers[33–35] did extensive work to bridge the gap, but rather used the Tomato Analyzer software, which may have calibration problems for pepper.

Furthermore, many factors, such as sharpness, focus, illumination influence, image angle, and distance between the object and sensor, influence the image acquisition and analysis, especially for RGB imaging of pepper[36,37]. More especially, spatial resolution is important for RGB-camera sensors to provide accurate information on the plants, and the distance between the object and the camera plays a major role[38]. Different camera distances have been used and recommended. For example, for a high-resolution image of ground maize at three-to-five leaf stages with faster-RCNN object detection algorithms, 0.3 cm and 0.6 cm image ground sampling distances were tested at an above-ground altitude ranging between 15.0 and 22.0 m using three different RGB cameras, Sony Alpha, DJI X7, and DJI Mavic 2 pro[39]. In another development, an enhanced sensor resolution and precision were achieved at a closed target using an RGB-D test at different light and distance levels[40]. For research on the use of smart sprayers for agricultural herbicide applications, the effects of camera selection (Canon T6 DSLR, LG G6 smartphone, and Logitech C920 webcam) and target distance (0.57 m, 0.98 m, and 1.29 m) on detection accuracy were tested on RGB images, and significant differences existed based on the camera selection and camera distances[41]. Other camera-to-object-distances, such as 1.0 m to study the effects of camera-shooting angle for 3D planting modelling with a multi-camera photography system[42], 1.0 m with an RGB camera, and 0.8 m with a thermal camera[43] have been reported. Furthermore, as low as 0. 27 m camera-to-object distance for leaf wetness measurements using laser-induced light reflection and RGB imaging[44] and then between 0. 25–0.40 cm for Time of Flight (active sensors) cameras and 0.75–0.85 cm for stereo vision cameras (passive sensors)[45] have also been used in other projects.

Those plant imaging studies do not show optimal or standard camera-to-object distances for a robust data acquisition for specific plant traits such as size, color and shape, especially for pepper, and how variations in distance influence plant imaging during growth. Therefore, studies on valid protocols are needed to standardize the camera-to-object distance in plant phenomics to increase accuracy, consistency and reproducibility of plant traits. These attempts will increase precision in image acquisition over the traditional system, particularly in addressing the variability in the imaging environment and ensuring consistency in the imaging process. For example, the introduction of automated focus adjustment, dynamic distance calibration, and 3D spatial mapping could maintain uniform image scale and clarity to enhance accurate quantitative traits extraction and interpretation across time points of plant phenology. Again, the various imaging parameters (For example, *Feret*, *Major*, *Minor*, and other imaging parameters) may have limitations to project specific actual plant traits (including growth in height, leaf area, fruit, and seed characteristics). However, these gaps are not well studied. This work provides a novel contribution by assessing the impacts of camera-to-object distance on imaging outputs, thereby identifying distance-sensitive biases and proposing a more reliable imaging protocol. This primary information will advance the methodological rigor in RGB imaging for a robust data acquisition in plant phenomics.

The study aims to determine the optimal camera-to-object distance for high-throughput RGB imaging of pepper plants at various growth stages, considering factors such as resolution and camera angle. By conducting a simple experiment, we intend to establish the best imaging setup to accurately analyze plant development, leaf morphology, fruits, and seed traits across four pepper accessions, three *Capsicum annuum* with different colors, and one *Capsicum frutescens*. Finally, our goal is to provide foundational insights that support advanced research into plant growth mechanisms and traits using high-throughput imaging systems, advancing precision and digital agriculture practices in open-field environments.

Materials and methods

Plant management

To maintain uniform color during crop image acquisition, the experiment was conducted in a greenhouse where temperature and light conditions were kept consistent. Four genotypes of pepper, including Kori, Caball, Oranzela (*Capsicum annuum* L.), and Red Pepper (*Capsicum frutescens* L.), were collected from the National Gene Bank, South Korea. The selection of the genotypes was only based on availability. The seeds were sown in a 50-cell seedling tray with one seed per cell. Ten seeds were sown per genotype. After two weeks of sowing, the seedlings were transferred into a 19 cm round seed pot filled with commercial soil (Bio-Sangto No.1 Premium, Farm Han Nong Co., Ltd., Seoul, The Republic of Korea). Five plants were kept for each genotype in a greenhouse at 25 ± 3 °C air temperature and 78% relative humidity. The length of photoperiod was automated and was adjustable between 8 and 16 h (approximately 16 h during the experimental period), providing an

average of 300 µmol m-2 s^{-1} photosynthetic photon flux density. After four and eight weeks of transplanting, NPK 15.15.15 at 0.45 g per plant was applied. During the fruit set, thrips (*Frankliniella occindentalis* (Pergande), order *Thysanoptera*) were spotted on the plants. The insects were checked with a 1:1 formulation of Captain (Fluxanethamide emulsion, Captain Insecticides, Gujarat, India) and bullet (Pleomethorine Lighuid, IndiaMart) every three days for two weeks.

Image acquisition

Imaging of the vegetative stage of the plants started two weeks after planting and was repeated weekly until the 6th week. Two imaging views were used, the top and the side views (Fig. 1), using a Sony camera (Sony ILCE-6000 with Sony E3.5/30 Macro lens, AVCHD 24.3 megapixels) at a 30 mm camera focal length and on an average of 23.5 × 15.6 sensor size. The camera settings included shutter speed at 1/8, aperture at 8.0, and light sensitivity at 500, but these settings were adjusted depending on the climatic conditions of the day. The camera tripod was fixed during measurements, and its position was adjusted according to plant growth for comparison. All the plants were used for the imaging and the exposure settings of the camera were held constant throughout the imaging process to minimize variability.

For the top view, the camera position above the plants was set at 0.6 m during the first three weeks and was later raised step-wise to 1.0 m as the plants grew. The imaging system utilized a Sony ILCE-6000 equipped with an APS-C sensor (23.5 × 15.6 mm) with an effective resolution of approximately 24.3 megapixels, resulting in images of 6000 × 4000 pixels and an estimated pixel size of approximately 3.9 µm. The camera-to-object distance was measured from the optical center of the camera lens to the central plane of the target object (e.g., leaves, fruits, and seeds), ensuring consistency across samples and clearly defining the imaging geometry. The camera was mounted on a stable support to preserve alignment and viewing angle, while the plant object positions were marked and maintained throughout the imaging process. A fixed white balance setting was used to prevent color shifts between images. Camera exposure parameters (shutter speed, aperture, and ISO) were kept constant during imaging to ensure exposure consistency. No post-acquisition brightness normalization was applied, as all images were captured under controlled lighting conditions. Imaging was conducted under controlled illumination to minimize shadows and reflections, using both top and side light-emitting diode (LED) grow lights with stable intensity and fixed positioning. This lighting setup ensured uniform brightness and color consistency across all images. In total, 100 images were acquired for the top view (4 cultivars × 5 plants × 6 weeks).

For the side view, three different distances between the plants and the camera (0.8 m, 1.0 m, and 1.2 m) were maintained for two angled images, 90 ° and 180 °. The three camera-to-object distances were selected based on the background information from Elsayed et al.[42], Lu et al.[43], and Xia et al.[46]. The camera, positioned at 1.0 m from the ground, was aligned parallel to the plant, forming a 90-degree angle with both the ground and the plant. A color checker with various color patches was included, and through color correction, identical color values were maintained across the images. The color checker also helped to convert image units from pixels to millimeters and later, to centimeters for further analysis. Six hundred side-view images were taken throughout the experimental time (4 cultivars x 5 plants x 2 imaging views x 5 weeks x 3 object-camera distance). A light-blue background was used for all the imaging as it is shown to provide better contrast for a segmentation process[47].

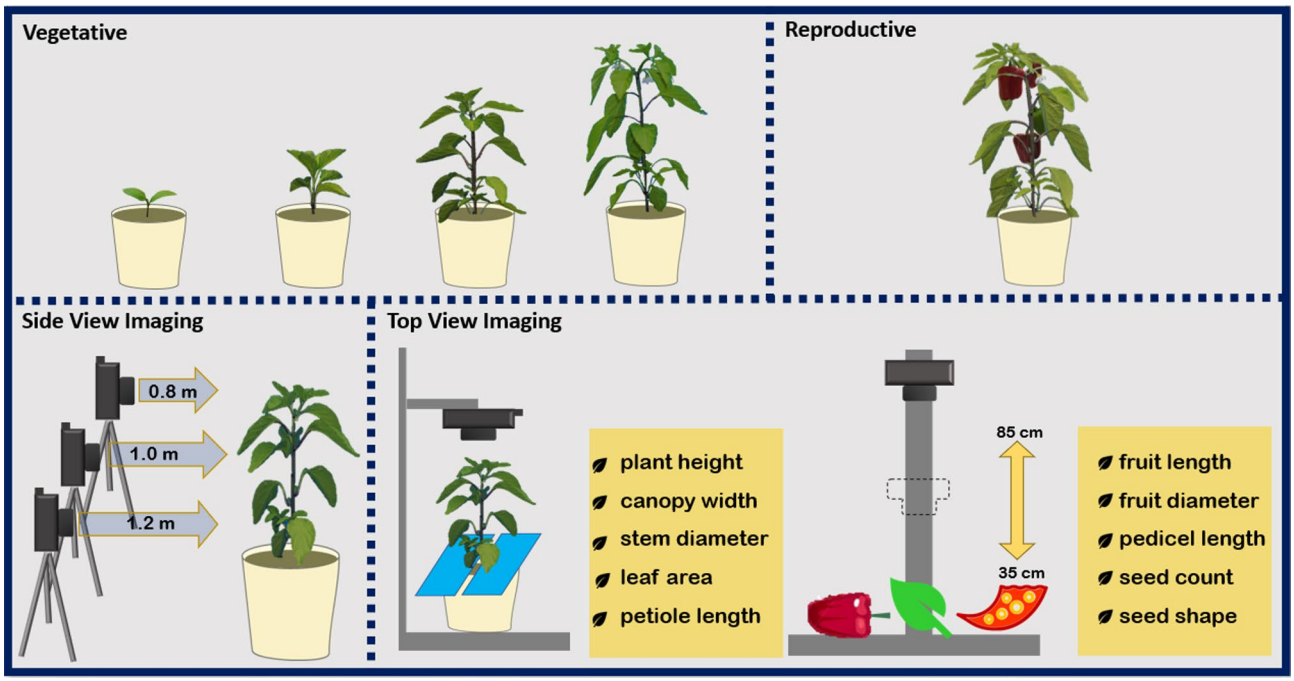


Fig. 1. Image acquisition and manual measurement methods.

After five weeks, three leaves per plant were harvested and imaged at four different camera-to-object distances, 0.55, 0.65, 0.75, and 0.85 m. This was repeated after the first fruit harvest. In total, 160 leaf images were taken (4 cultivars x 5 plants x 2 imaging times x 4 imaging distances). Each leaf image had three leaf samples, making a total of 480 individual leaf images. At the reproductive stage, between 2 and 3 fruits were harvested per plant and imaged at five different camera distances, 0.45, 0.55, 0.65, 0.75 and 0.85 m. About 60 individual fruit images were taken. After the whole fruit imaging, the seeds per fruit were dried at room temperature for 5 days and also imaged. About sixty seed images from the individual fruits were also targeted, and 1720 individual seed data points were collected. On average, 105 ± 50 seeds were extracted per fruit from Caball, 58 ± 31 from Kori, 142 ± 63 from Oranzela, and 38 ± 20 from Red pepper genotypes.

The image format was collected in RAW and calibrated using the X-Rite Color Checker as a color reference. The calibrated images were converted to JPEG for image processing.

Image processing

The processing of the images was based on the algorithms from the ImageJ program using an extension script (macron created locally). Two folders, named *input* and *output*, were created and used for the analysis. Images for analysis were saved in the input folder. When the image software was launched, the script and the images of the plant were dragged into ImageJ, and the image segmentations followed. The background noise was separated using the YUV model in the *Color Threshold* window in the *Adjust* command of the *Image* window (Fig. 2). On average, the Y was set at 0 and 255, U at 0 and 132 (which would vary across the plant organs, but we focused on background color rather than adjusting individual object thresholds), and then V at 0 and 255 to separate the background noise. A line picker was used to draw a line from one end to the other end (a 10 mm mark) of one of the color checkers of the scale bar to calibrate the units from pixels to millimeters. On average, the distances in pixel to SI unit scale calibration were maintained at 94.02 pixels/10 mm for 0.8 m, 77.35 pixels/10 mm for the 1.0 m and 67.01 pixels/10 mm for the 1.2 m camera-to-object distance for the side view imaging. For the top view imaging of all the plant parts, the scale calibration ranged from 324.00 pixels/10 mm for the 0. 45 m to 164 pixels/10 mm for the 0. 85 m camera-to-object distances. The color checker on the scale bar which was closer to the plant object of interest was always selected for the scale setting. After the calibrations, a measurement area was selected using the rectangular or oval picker, and the background color was adjusted to blue. A limited object size of 300 mm for plant analysis and 1 mm for seeds and fruits was set to exclude other background particles that may be wrongly picked for analysis. After these changes, the script was run on the data. A similar application was used for the side views and the reproductive parts.

Output from the image J program, including *Height*, *Feret*, *Major*, *Minor*, *Width and Area*, was further analyzed using the R statistical software version 4.4.0. A correlation was established between manual measurements and imaging data to identify which of the traits from the imaging data would explain the manual measurements well.

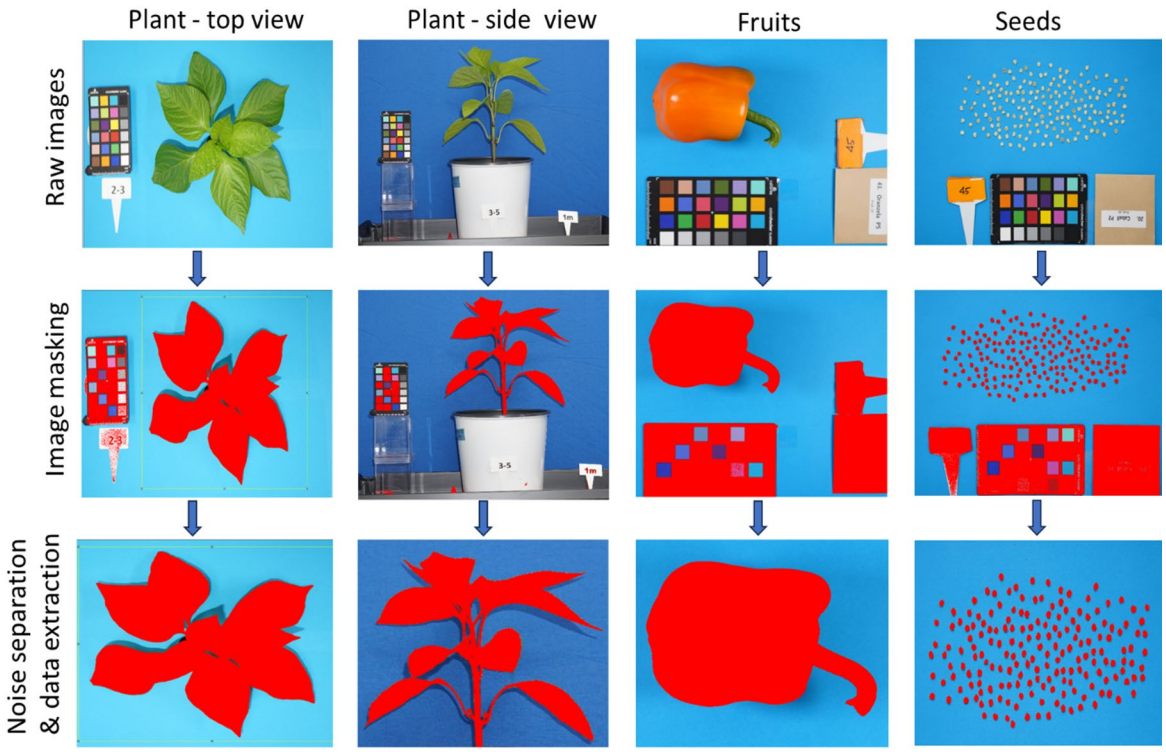


Fig. 2. Image analysis processes of the plants using ImageJ software.

Manual measurements

During every week of image acquisition, plant height, stem diameter, and canopy spread were measured manually (Fig. 1). Plant height was measured from the soil surface to the highest part of the plant. Stem diameter was measured 2 cm from the soil surface, while canopy spread was measured from the widest part of the top-view of the plant. Again, leaf area was measured with a leaf area meter (Licor, Model LI-3100 Area Meter) while leaf length and width were measured with a meter rule. Fruit width was measured with a vernier caliper, while fruit length was measured with a meter rule. After imaging, the seeds were extracted at full ripening and dried for 5 days at room temperature and weighed. The individual fruits were also cut into pieces and then oven dried at 70 °C to a constant weight and weighed.

Data analysis

For the vegetative studies of top view and side view, a correlation analysis was used to identify the best image parameter to study plant height and canopy spread. For the distance effect of the side view, a repeated-measure analysis was employed using the linear mixed effects model in R version 4.4.0[48]. The model included the fixed effects of Genotype (G), Distance (D), and Time (T) as well as their interactions (GDT), and the random effects of the number of plants/leaves/fruits used (pl) and the other error terms (ε).

$$Y_{(repeated\ measurments)} = \alpha\ (G) + \beta\ (D) + \gamma\,(T) + \mu\ (GDT) + \mathrm{A}\,(pl) + \varepsilon$$

Genotype and distance were used as the fixed factors for leaves and fruits, while the number of plants and leaves or fruits were used as the random effects. For which parameter to measure, and based on which actual measurements, a correlation analysis was performed using specific distances, thereby separating the data into respective distances and correlating the actual measurements with the image parameters. For seed analysis, the responses of different genotypes were studied through the analysis of variances using the *Agricolae* package[49]. The normality of the data was checked using the normal distribution plots, quantile-quantile plots, and histogram distribution plots. For fruit analysis, *Area*, *Minor*, and fruit height were power transformed, while for seeds analysis, *Solidity* was also power transformed. *Circularity* and *Roundness* were square-root transformed, while the *Aspect Ratio* was log-transformed to determine significant differences. The mean separation was done using the Tukey Honest Significant Differences (Tukey HSD) at the 0.05 probability level.

Results

Vegetative—top view

We compared *Height*, *Feret*, *Major*, *Minor*, *Width*, and *Area* from the imaging analysis with the canopy diameter measured with a meter rule, a correlation coefficient ranging from 0.79 to 0.84 and RMSE between 6.50 and 73.51 were identified (Fig. 3). The *Major* ($R = 84$, RMSE = 10.37) and the Feret parameters ($R = 0.82$, RMSE = 6.50) showed the highest correlation and the least RMSE values while *Perimeter* ($R = 79$, RSME = 73.51) showed the least correlation and highest RMSE with the actual canopy diameter.

When the actual measurement of canopy spread was plotted with *Major* (the imaging parameter), a similar pattern of growth was identified; however, we identified about 5–10 cm growth differences among all the genotypes (Fig. 4).

Plant growth with time also affected the precision of the comparison between the physical measurement and the *Major* (image measurement of canopy spread). The divergence of the graphs was more pronounced 6 days after planting compared with two days after planting. The reduction in sensitivity was more pronounced in Kori, Oranzela, and Red pepper than in Caball.

Vegetative—side view

For the side-view imaging, plant height from imaging was similar to the actual height measurement, with a 0.90 correlation and 10.64 RMSE. Unlike the top view, the side view canopy spread correlated with *Minor* than *Major* (Fig. 5). Generally, the correlation of actual plant height with the imaging parameters ranged from 0.7 to 0.9. For canopy spread, the correlation coefficient was between 0.7 and 0.87.

Selecting image *Height* and *Minor* as the two parameters to study actual plant height and canopy spread, the three camera-to-object distances gave different correlations among the genotypes (Table 1). The analysis of variance also showed a significant difference in the distance effect on imaging of height ($P = 0.001$) and imaging of canopy spread (Minor) ($P = 0.0319$) at the selected camera-to-object positions. Generally, the further the object is from the camera, the lower the representation of the measurements through imaging. The 0.8 m camera-to-object distance gave a strong correlation and RMSE values among the four genotypes for both plant height and canopy spread.

Vegetative—leaf parameters

Highly significant differences existed ($P < 0.001$) using the selected distances (0.55–0.85) to image the leaves of the pepper genotypes (Supplementary Table S1). The 0.55 m and the 0.65 m showed better performances than the 0.75 m and 0.85 m (Table 2). Leaf length was better measured by *Height*, *Feret*, and *Major* with a 0.95 correlation. Similar observations were shown on leaf diameter with a correlation coefficient of 0.89. Leaf area was rather reflected by *Feret* and *Major* with a 0.86 correlation, while the correlation value appeared 0.81 for image *Area*.

Reproductive—fruits

The camera-to-object distances of 0.55 m and 0.65 m are suitable for fruit measurements based on correlation. On the other hand, the analysis of variance did not show significant differences in distance effects on the parameters

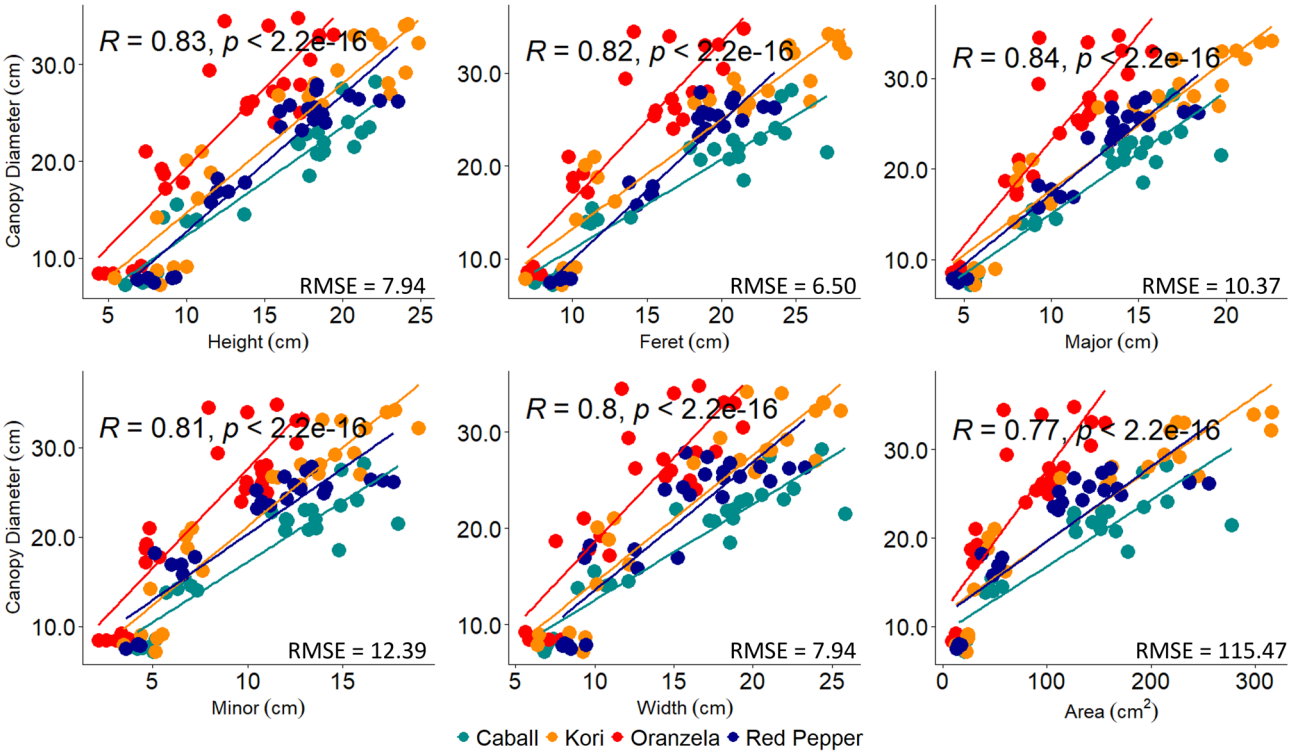


Fig. 3. Correlation between canopy spread from manual measurements and *Height*, *Feret*, *Major*, *Minor*, *Width*, *and Area* parameters from automated measurements. The R-value is the correlation coefficient, while *p* is the probability level at 0.05, and RMSE is the root mean square error. High R and low RMSE values show precision in using imaging parameters to predict the actual measurements, $n = 100$.

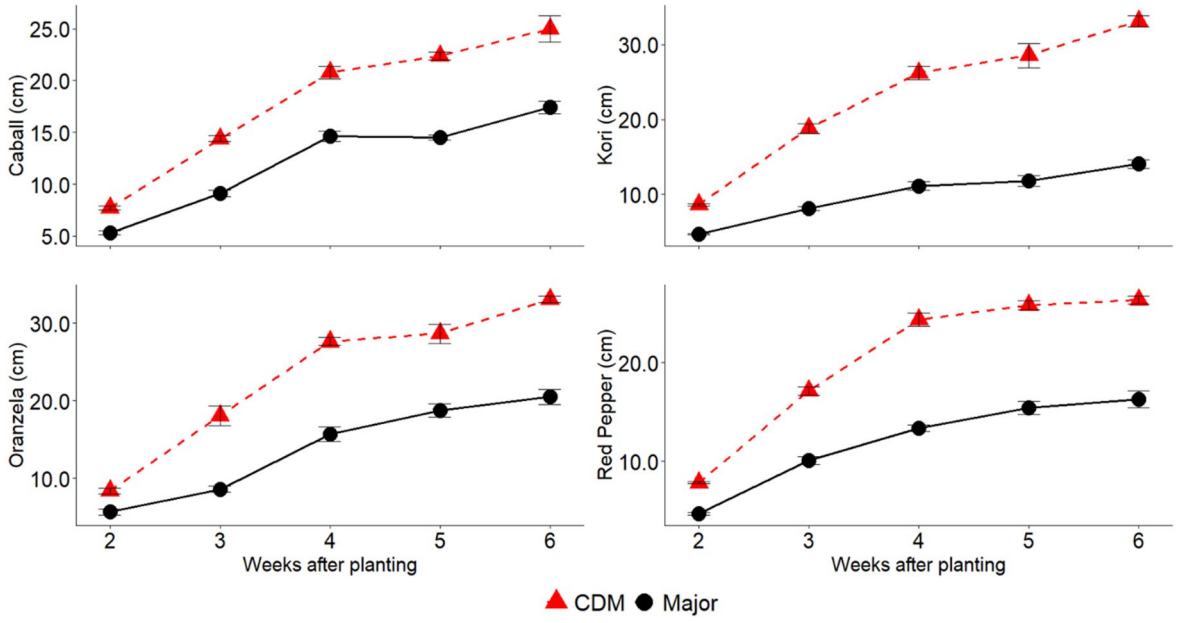


Fig. 4. Plant area spread - *Major* (an imaging parameter) versus canopy diameter (CDM) (actual measurement).

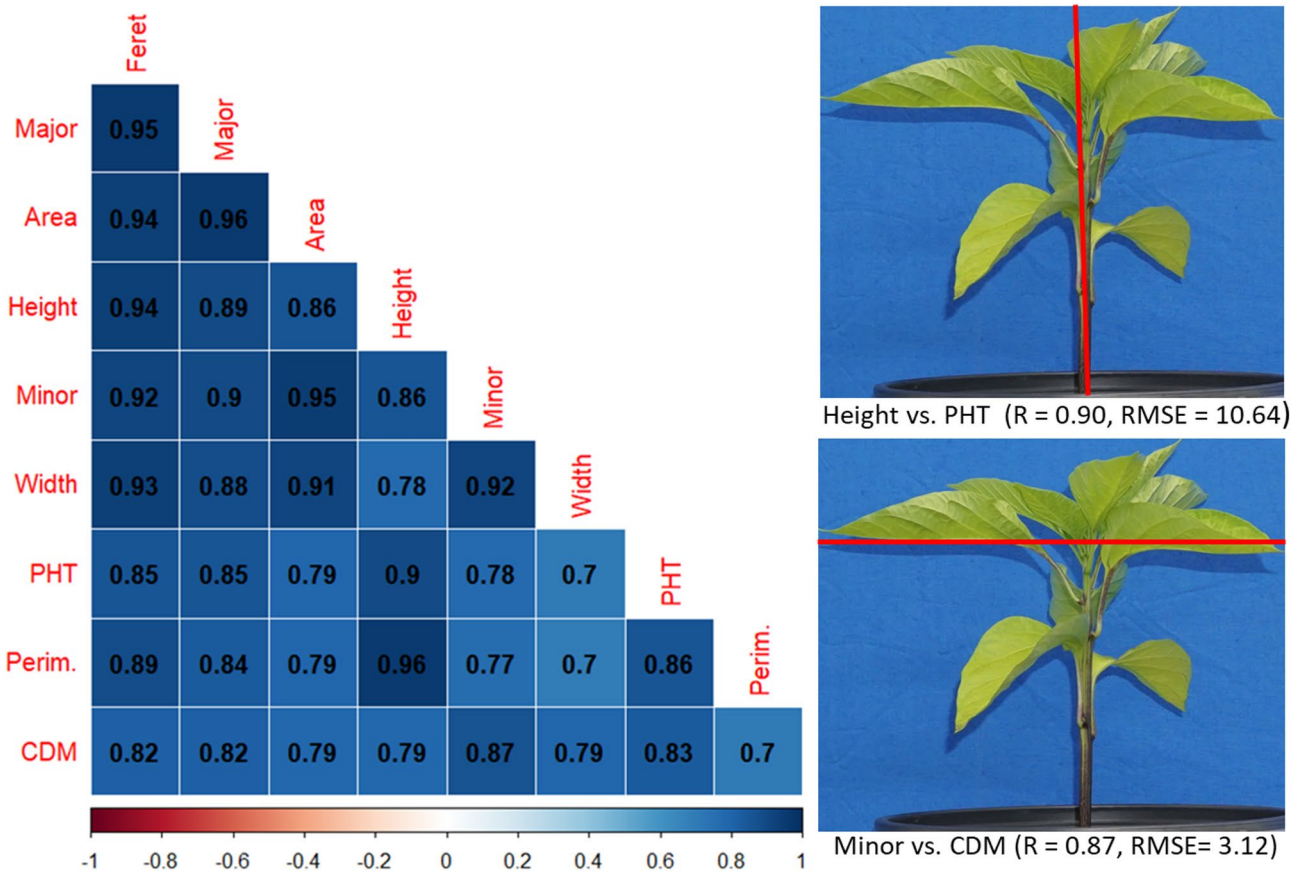


Fig. 5. Correlation between image parameters (*Height*, *Feret*, *Major*, *Minor*, *Width*, *Area*, *and Perimeter*) and manual measurements (PHT and CDM), PHT – Plant Height, CDM – Canopy diameter. $n = 600$.

(Supplementary Table S1). Fruit length was improved with *Feret* by 0.87 correlations at a 0.65 m distance. Fruit diameter, on the other hand, correlated strongly with *Minor* with a 0.90 correlation at 0.55 m. Also, fresh and dry weights showed 0.94 and 0.89 correlation with image *Area* at 0.55 m, respectively (Table 3).

For the four genotypes studied, red pepper was the only chili pepper (*Capsicum frutescens* L.) type, while the other three (Caball, Kori, and Oranzela) were the sweet pepper types (*Capsicum annuum* L.). Red pepper had red, elongated fruits with obtuse shapes at the pedicel attachment and pointed at the blossom end. On the other hand, the sweet pepper types had yellow, red, and orange mature fruits with blocky shapes, cordate at the pedicel attachment, and sunken at the blossom end. The actual measurement of plant height of the four genotypes reflected on *Major* and *Feret*, while fruit diameter, fresh weight, and dry weight from manual measurements gave similar patterns with *Area* and *Minor* (Fig. 6). *Major* and *Feret* provided similar information on fruit measurements compared with the other parameters. Caball, Kori, and Oranzela showed similar fruit characteristics apart from the matured fruit color, in which Caball was yellow, Kori was red, and Oranzela was orange. Imaging *Height* and *Major* for Red Pepper were similar, and almost similar for the other genotypes. The Oranzela fruits showed the highest variability in terms of image *Area* and thus reflected on the fresh and dry weights of the genotype. On the other hand, the actual measurement of fruit height was more variable in Kori, while Red Pepper fruits were more variable for *Feret* measurements.

Reproductive—seeds

After different distance trials, ranging from 0.35 to 0.85 m, we identified 0.55 m and 0.65 m to have a good correlation with seed diameter measured manually. The 0.65 m distance was finally selected for other analysis since it was comparatively better. For the four genotypes studied, different seed characteristics were identified based on the imaging results. Oranzela seeds were bigger among the four, but compared with Kori, it had lower solidity (Table 4). Red pepper had small seeds. Caball, Kori, and Oranzela seeds showed better circularity and roundness than red pepper. On the other hand, Caball seeds were more round among the four genotypes. Seeds from red pepper showed the highest aspect ratio, followed by Kori and Oranzela.

Discussion

This study examined the effects of imaging parameters and camera-to-object distances for plant growth characterization, emphasizing non-destructive monitoring of plant phenology. *Major* parameters proved most effective for measuring canopy spread in top-view imaging, while *Minor* parameters were better suited for side-

Genotypes	Distance (m)	*r*	95% CI	df	RMSE
Image height vs. Actual height					
Caball	0.8	0.98	0.94–0.99	18	7.28
	1.0	0.96	0.91–0.98	23	8.62
	1.2	0.90	0.79–0.96	23	10.23
Kori	0.8	0.94	0.85–0.98	18	7.44
	1.0	0.94	0.86–0.97	23	9.63
	1.2	0.86	0.70–0.93	23	10.87
Oranzela	0.8	0.95	0.87–0.98	18	7.03
	1.0	0.94	0.86–0.97	23	9.28
	1.2	0.84	0.67–0.93	23	11.53
Red Pepper	0.8	0.98	0.95–0.99	18	7.44
	1.0	0.96	0.90–0.98	23	11.39
	1.2	0.94	0.87–0.973	23	12.61
Image canopy spread (*Minor*) vs. Actual canopy spread					
Caball	0.8	0.96	0.91–0.99	18	3.58
	1.0	0.92	0.82–0.96	23	3.88
	1.2	0.84	067–0.93	23	3.26
Kori	0.8	0.94	0.86–0.98	18	1.87
	1.0	0.90	0.79–0.96	23	1.96
	1.2	0.83	0.65–0.92	23	1.71
Oranzela	0.8	0.92	0.81–0.97	18	3.58
	1.0	0.89	0.77–0.95	23	4.50
	1.2	0.84	0.66–0.93	23	3.42
Red Pepper	0.8	0.93	0.83–0.97	18	3.32
	1.0	0.95	0.89–0.98	23	3.30
	1.2	0.93	0.85–0.97	23	2.39

Table 1. Object-to-camera distance effects on the correlation between actual measurement of plant height and canopy spread. Where *r* Pearson correlation coefficient, *CI* Confidence interval, *df* Degree of freedom, *RMSE* Root mean square error.

Actual Measurements	Image Measurements *n* = 480					
Camera-Object Distance	Height	Feret	Major	Minor	Width	Area
0.55 m						
Leaf Length	0.95	0.95	0.95	0.83	0.85	0.89
Leaf Diameter	0.88	0.89	0.89	0.81	0.84	0.85
Leaf Area	0.83	0.86	0.86	0.73	0.78	0.81
0.65 m						
Leaf Length	0.94	0.94	0.93	0.78	0.8	0.86
Leaf Diameter	0.89	0.90	0.9	0.78	0.82	0.84
Leaf Area	0.85	0.85	0.85	0.69	0.71	0.79
0.75 m						
Leaf Length	0.93	0.93	0.91	0.73	0.75	0.81
Leaf Diameter	0.89	0.89	0.89	0.75	0.79	0.82
Leaf Area	0.84	0.83	0.82	0.64	0.67	0.75
0.85 m						
Leaf Length	0.86	0.86	0.85	0.67	0.69	0.75
Leaf Diameter	0.86	0.85	0.85	0.71	0.75	0.76
Leaf Area	0.78	0.77	0.77	0.59	0.62	0.67

Table 2. Object-to-camera distance effects on the correlation between actual measurement of leaf dimensions and image parameters.

Actual Measurements	Image Measurements $n=60$								
Camera-Object Distance	Height	Feret	Major	Minor	Width	Area	solidity	AR	Round
0.45 m									
Fruit Length	0.24	0.57	0.52	0.35	0.58	0.43	−0.15	0.22	−0.21
Fruit Diameter	0.62	0.46	0.40	0.66	0.46	0.55	−0.02	0.44	0.36
Fruit Fresh weight	0.45	0.59	0.56	0.56	0.58	0.58	−0.02	0.01	0.01
Fruit dry weight	0.35	0.51	0.44	0.41	0.51	0.43	−0.19	0.03	−0.03
0.55 m									
Fruit Length	0.64	0.83	0.82	0.67	0.80	0.76	−0.07	0.33	−0.30
Fruit Diameter	0.89	0.78	0.75	0.90	0.74	0.87	0.08	−0.22	0.27
Fruit Fresh weight	0.87	0.92	0.91	0.88	0.88	0.94	−0.01	0.11	−0.08
Fruit dry weight	0.82	0.86	0.87	0.81	0.82	0.89	0.02	0.14	−0.11
0.65 m									
Fruit Length	0.60	0.87	0.84	0.64	0.85	0.80	0.23	0.29	−0.30
Fruit Diameter	0.86	0.62	0.61	0.83	0.59	0.80	−0.03	−0.30	0.32
Fruit Fresh weight	0.80	0.84	0.85	0.81	0.80	0.92	−0.07	0.06	−0.07
Fruit dry weight	0.73	0.77	0.75	0.73	0.73	0.82	−0.19	0.02	−0.03
0.75 m									
Fruit Length	0.60	0.80	0.79	0.65	0.78	0.79	−0.16	0.23	−0.23
Fruit Diameter	0.85	0.62	0.61	0.83	0.58	0.81	−0.01	−0.31	−0.34
Fruit Fresh weight	0.81	0.82	0.85	0.85	0.78	0.94	−0.02	0.02	−0.02
Fruit dry weight	0.72	0.75	0.73	0.71	0.72	0.81	−0.20	0.03	−0.04
0.85 m									
Fruit Length	0.60	0.78	0.78	0.64	0.78	0.78	−0.17	0.23	−0.17
Fruit Diameter	0.83	0.61	0.60	0.82	0.58	0.79	−0.01	−0.31	0.34
Fruit Fresh weight	0.81	0.81	0.83	0.84	0.77	0.93	−0.02	0.02	−0.02
Fruit dry weight	0.71	0.74	0.72	0.71	0.71	0.80	−0.20	0.03	−0.20

Table 3. Object to camera distance effects on the correlation between actual measurement of whole fruit dimensions and image parameters.

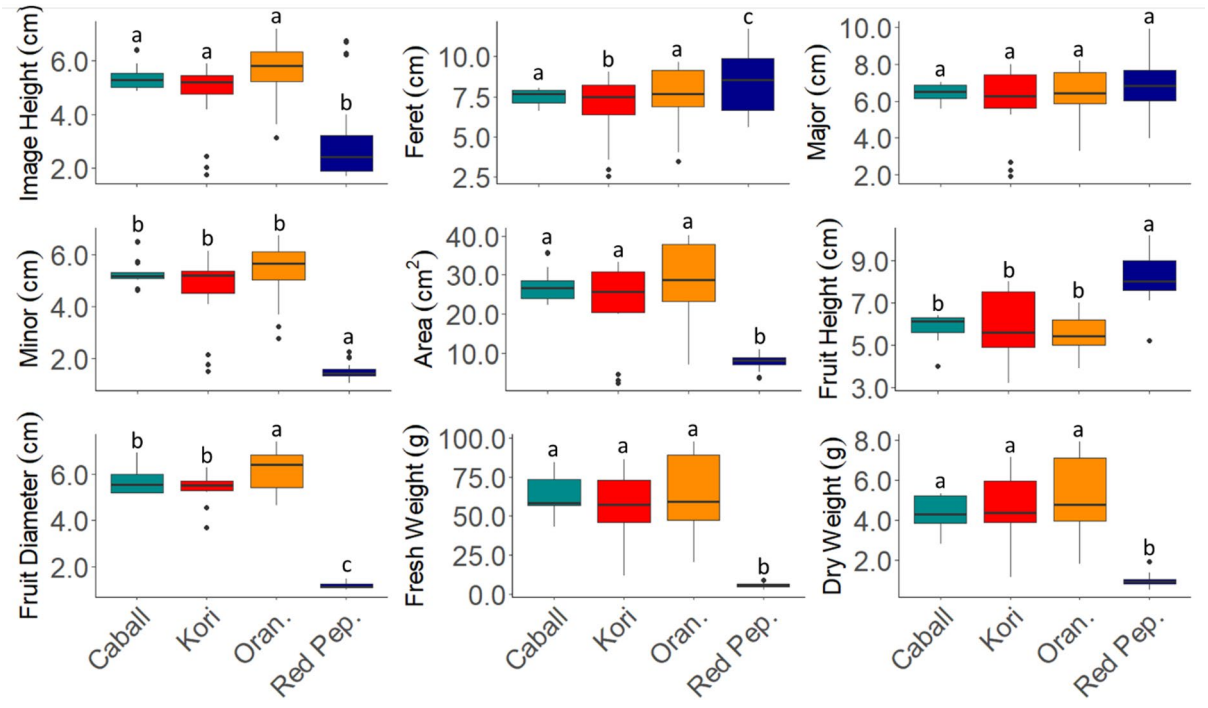


Fig. 6. Box plot of fruit characteristics of the different genotypes of pepper from image parameters and manual measurements. Significant differences: *Area*, *Minor*, Fruit height, Image *Height*, Fruit diameter, Fruit fresh weight, and Fruit dry weight ($P=0.000$), Major ($P=0.3429$), and Feret ($P=0.001$), $n=60$.

Traits	Caball	Kori	Oranzela	Red Pepper	$P_{(0.05)}$
Height (mm)	1.87 ± 0.15c	1.90 ± 0.15b	1.94 ± 0.12a	1.76 ± 0.14d	< 0.001
Feret (mm)	2.00 ± 0.12c	2.04 ± 0.12b	2.06 ± 0.10a	1.92 ± 0.11d	< 0.001
Major (mm)	1.94 ± 0.0.12c	1.99 ± 0.12b	2.03 ± 0.09a	1.87 ± 0.10d	< 0.001
Minor (mm)	1.69 ± 0.11c	1.71 ± 0.11b	1.74 ± 0.09a	1.56 ± 0.11d	< 0.001
Width (mm)	1.85 ± 0.14c	1.89 ± 0.14b	1.93 ± 0.13a	1.78 ± 0.15d	< 0.001
Area (mm^2)	2.58 ± 0.32c	2.67 ± 0.31b	2.78 ± 0.25a	2.30 ± 0.26d	< 0.001
Solidity	0.96 ± 0.01b	0.97 ± 0.01a	0.96 ± 0.01b	0.96 ± 0.01b	< 0.001
Circularity	0.85 ± 0.02a	0.85 ± 0.02a	0.85 ± 0.02a	0.84 ± 0.03b	< 0.001
Roundness	0.87 ± 0.03a	0.86 ± 0.03b	0.86 ± 0.03b	0.83 ± 0.05c	< 0.001
Aspect Ratio	1.15 ± 0.05c	1.16 ± 0.04b	1.16 ± 0.04b	1.21 ± 0.08a	< 0.001

Table 4. Seed characteristics of the genotypes at 0.65 m. Means in a row with the same letters are not statistically significant. Means are ± the standard deviation of the means, $n = 1720$.

view assessments. Similar findings by Igathinathane et al.[50] showed that *Major* and *Minor* parameters effectively determine particle dimensions, especially for shapes approximating circles and ellipses. Polder et al.[51] also reported strong correlations between *Major* and *Minor* axes and seed dimensions, illustrating their utility across different views. Both top and side-view imaging capture canopy spread within a curvilinear framework, with these parameters representing the primary and secondary axes of the best-fitting ellipse. Notably, the secondary axis may be more prominent in side views, whereas the primary axis dominates in top views. Further research is necessary to understand the reasons behind these differences, optimize imaging approaches for plant trait measurement.

The imaging parameters had different interpretations from the actual plant measurements. As we have already explained, *Major* and *Minor* measured well the canopy diameter, and *Height* measured well plant height with side view imaging. Plant height and stem diameter are important traits to determine plant growth. The two parameters determine the ability of plants to compete for light and to facilitate photosynthesis[52,53]; therefore, an efficient and accurate way to measure the parameters is important. Different imaging methods have been employed to measure height[54], and these findings provide baseline information on the imaging parameters that can be used to represent height with precision. Measurement of plant height using imaging has also been confirmed by Treder et al.[55] on pear trees, Polter et al.[56] on aquatic plants, and Brunes et al.[57] on wheat seedlings.

For leaf characteristics, leaf length, width, and area were better measured by *Major*, *Minor*, *Feret*, and *Area* than the other parameters. The orientation of the leaf might be a contributing factor for the measurements as *Major* (the longest line that can be drawn within the leaf), *Minor* (the shortest line perpendicular to the major axis), and *Feret diameter* (the longest distance between any two selected points along the leaf perimeter) better account for irregular shapes and variations in particle orientations[50]. The leaves are important organs for plant activities, which are involved in light capture, gas exchange, photosynthesis, and other important functions[58]. The *Major*, *Minor*, and *Feret* would offer a more adaptable approach to capture varying shapes and orientations of different leaf species. Measuring leaf dimensions, especially the leaf area, is mostly done through the destructive method using a leaf area meter or other devices[59], but the imaging approach can be easy, more accurate, and more precise than the traditional approach, aside from being non-destructive. Further research in the imaging approach can provide a non-destructive method with precision and accuracy, and the leaves can be studied over a long time.

More so, actual measurement of fruit length correlated well with *Feret*, while *Minor* and *Height* well-calibrated fruit diameter. A good relationship existed between fruit fresh and dry weights with image *Area* than all the other parameters. These observations provide information on what imaging parameter is needed for a particular trait of the plants. Few attentions are given to these observations in the phenotypic analysis of plants. Fruit segmentation of the different pepper cultivars needed some levels of care and precision. More especially, the red pepper has some dark brown spots around the point of attachment to the pedicel. Much attention was needed for the masking and the segmentation. Moreover, weak correlations were identified among some of the traits, which could be due to the trait differences among the genotypes that were not considered in some of the analyses. Further research is needed here.

The experiment provided information on the effect of distance on the imaging of the plants. Generally, the short camera-to-object distances provided better correlations than the long distances. The camera-to-object distance plays a crucial role in providing accurate data for RGB-camera sensors[38]. The camera-to-object distance can affect the sharpness and the resolution of the images, which can cause wrong image interpretations. As the plant grows, image resolutions change and thus affect the camera-to-object distance. For the side-view imaging of the vegetative growth of the plants, the 0.8 m camera-to-object distance was identified to produce a higher correlation between the image parameters and the actual measurements compared with the 1.0 and 1.2 m. The observation could result from spatial resolution, pixel density, and object scale relative to the camera's field of view. Decreasing or increasing camera-to-object distance affects pixel density on the object and the texture complexity of the plant organs (such as leaves, flowers, and fruits). Beyond 0.8 m, a few pixels might have been occupied for traits extraction and segmentation, but measurement noise might have increased. Other factors might result from perspective distortion and increased occlusion among the plant organs. At 0.8, plant architecture might have balanced the frame to maintain enough pixels for trait extraction. On the other hand, handling the short

distance is difficult when the plants are fully grown, as the camera coverage reduces, and therefore misses some parts of the plant. In this way, increasing the camera distance step-wise may be appropriate to study the overall life span of the plant.

For leaves, fruits, and seeds, imaging at 0.55 m and 0.65 m object-to-camera distances was better than the very short distances of 0.35 and 0.45 m, and the long distances of 0.75 and 0.85 m. However, some of the parameters depended on a particular distance selection. For example, Fruit length measured manually was improved with *Feret* by 0.87 correlations at 0.65 m camera-to-object distance, while fruit diameter measured manually correlated strongly with *Minor* (0.90 correlation coefficient) at 0.55 m camera-to-object distance. Hennessy et al.[41] demonstrated significant differences in the camera-to-object distances in the RGB detection accuracy of agricultural herbicide applications. Different camera distances, mostly ranging between 0.25 and 1.0 m, have been employed for plant image analysis. Frogeye leaf spots on soybeans were studied with a 0.75 m camera-to-object distance[60], while as low as 0.27 m camera-to-object distance was used for leaf wetness studies[44]. This work provides primary information on the need for optimal and standard camera-to-object distances for controlled and open field plant imaging.

The seeds of the four pepper genotypes studied showed different characteristics based on the imaging parameters. Oranzela seeds had better imaging parameters, such as *Height*, *Feret*, *Major*, *Minor*, *Width*, and *Area*, while red pepper had the least. In real terms, Oranzela seeds were bigger while red pepper seeds were smaller. Caball, Kori, and Oranzela seeds showed better *Circularity* and *Roundness* than red pepper, which also had the maximum *Aspect Ratio*. Thus, Red pepper seeds adjust better to an ellipse than a circle, as reported by Martin-Gomez et al.[61] in Castor Beans. *Circularity* values range from 0.0 to 1.0, and the closer the value is to 1, the perfect the circle shape of the seeds[62]. *Roundness*, on the other hand, measures how the shape of the seed is close to a perfect circle[63], and it is the inverse of the *Aspect Ratio*. *Aspect Ratio* is the proportion relationship between the maximum and minimum *Feret Diameter* (the caliper diameter)[64], which provides information on the degree to which the pepper seeds are stretched. *Roundness* can exist in more than one plane, as *Circularity* exists in one plane. Also, *Solidity* provides information about the smoothness of the curves of the seeds, and it describes the degree to which the projected contour of the pepper seeds is concave[65,66].

The closer the *Solidity* is to 1, the more the projected contour is to its convex hull[67], and the fewer the projections, depressions, and rough corners on the seed surface. This means the Red Pepper seeds may comparatively be small, flat, stretched, and with surface projections than the other genotypes. Arredondo-Valdez et al.[63] utilized *Roundness*, *Circularity*, and *Aspect Ratio* to assess the quality of Opuntia ficus-indica seeds and confirmed the accuracy of using these parameters in seed studies. Seed characterization through imaging provides numerous characteristics for comparison, which can aid in seed differentiation, a process that wouldn't be possible with manual methods. Also, the precision of using images is higher than the manual methods[64]. This observation is based on studies done in a controlled environment.

The imaging approach of phenotyping can support the traditional method and can help speed up the selection of different plant traits for further improvements. Imaging is less laborious, non-destructive, can capture a wider range of traits at a plant growth period, and reduces human error in data acquisition. There are more recent reviews on phenotyping standards and best practices to guide the use of automated methods for plant phenotyping[68,69]. This experiment has shown that imaging can be used at different stages of the plant.

It is noted that some challenges, such as occlusions, light effects, and robust growth of different varieties, occur in plant imaging[70]. Furthermore, the 2D RGB images reduce detailed information on a three-dimensional plant organ, such as fruits, due to a single viewpoint. In view, only the projected area of the visible organs is captured while discriminating against the hidden traits. This leads to reduced pixel intensity and causes underestimation of the plant traits, thus affecting the correlation between projected and actual measurements. Additional imaging experiments could help increase segmentation accuracy while reducing noise in shape- and texture-based metrics. The comparison of the analysis tool with the real measurements needs expansion to involve different plant data to ensure its reliability and validity[71]. Further work in this research dimension will provide the overall picture of using imaging tools for plant analysis to provide a broader picture of plants' genetic traits and the definition of the traits by their environmental conditions. The imaging approach affords an efficient and possible way to link the genotype to the phenotype to select high-yielding and stress-tolerant plants[72,73]. RGB imaging is continuously used in plant studies, including seed morphology, germination rates, seedling vigor, root architecture, shoot biomass, and yield traits[73–75].

Conclusion

RGB imaging could offer a reliable, non-destructive alternative for the practical measurement and characterization of plant traits. In this study, imaging parameters such as *Major*, *Minor*, and *Feret diameter* from ImageJ effectively captured traits including plant height, canopy spread, and organ dimensions, while seed traits like *Roundness*, *Circularity*, and *Solidity* highlighted metabolic diversity among pepper genotypes. Camera distance significantly influences image resolution and accuracy especially in a controlled environment; a distance of 0.8 m is optimal for vegetative stages, whereas 0.55–0.65 m is recommended for fruit, leaf, and seed imaging to achieve high correlation with actual measurements. The advantages of RGB imaging over traditional methods include its adaptability to irregular plant shapes and its non-destructive nature. The imaging could, however, not solve the challenges of some plant organs overlapping the others, especially for vegetative imaging due to the complex architecture of the plants. Again, using the two-dimensional imaging to study fruit characteristics (a three-dimensional object) was not very efficient and needs improvement. Further research is necessary to refine imaging parameters for specific plant traits and developmental stages, enhancing the application of high-throughput imaging in precision agriculture.

Data availability

Data will be available upon request to the corresponding author, Jeongho Baek.

Received: 2 September 2025; Accepted: 26 March 2026
Published online: 05 April 2026

References

1. Santos, T. et al. Characterization and diversity of peppers (*Capsicum* spp.) genotypes based on morphological traits using multivariate analysis. *Journal of Experimental Agriculture International* **39**(1), 1–10. https://doi.org/10.9734/jeai/2019/v39i130325 (2019).
2. Tripodi, P. & Greco, B. Large-scale phenotyping provides insight into the diversity of vegetative and reproductive organs in a wide collection of wild and domesticated peppers (*Capsicum* spp.). *Plants* **7**(4), 103. https://doi.org/10.3390/plants7040103 (2015).
3. Pereira-Dias, L., Vilanova, S., Fita, A., Prohens, J. & Rodriguez-Burrueso, A. Genetic diversity, population structure, and relationship in a collection of pepper (*Capsicum* spp.) landraces from the Spanish centre of diversity revealed by genotyping-by-sequencing (GBS). *Hortic. Res.* **54**, 1–13. https://doi.org/10.1008/s41438-019-0132-8 (2019).
4. DeWitt, D. & Bosland, P. W. *Peppers of the world: An identification guide* (Ten Speed Press, 1996).
5. Onus, A. N. & Pickersgill, B. Unilateral incompatibility in *Capsicum* (Solanaceae) occurrence and taxonomic distribution. *Ann. Bot.* **94**, 289–295. https://doi.org/10.1093/aob/mch139 (2004).
6. Kraft, K. H. The domestication of the Chilli Pepper, Capsicum annuum: Genetic, Ecological and Anthropogenic Patterns of Genetic Diversity. ProQuest Dissertation and Theses. (2009).
7. Olatunji, T. L. & Afolayan, A. J. The suitability of chili pepper (*Capsicum annuum* L.) for alleviating human micronutrient dietary deficiencies, a review. *Food Sci. Nutr.* **6**(8), 2239–2251. https://doi.org/10.1002/fsn3.790 (2018).
8. Nicolai, M., Cantet, M., Sage-Palloix, L. V., Palloix, A. & A. M., and Genotyping a large collection of pepper (Capsicum spp) with SSR loci brings new evidence for the wild origin of cultivated C annuum and the structuring of genetic diversity by human selection of cultivar types. *Genet. Resour. Crop Evol.* **60**, 2375–2390. https://doi.org/10.1007/s10722-013-0006-0 (2013).
9. Moses, M., Umaharan, P. & Dayanandan, P. Microsatellite based analysis of the genetic structure and diversity of *Capsicum chinensis* in the Neotropics. *Genet. Resour. Crop Evol.* **61**, 741–755. https://doi.org/10.1007/s10722-013-0069-y (2014).
10. Lee, H. Y. et al. Genetic diversity and population structure analysis to construct a core collection from a large *Capsicum* germplasm. *BMC Genet.* https://doi.org/10.1186/s12863-016-0452-8 (2016).
11. Dalal, A. et al. Dynamic physiological phenotyping of drought-stressed pepper plants treated with productivity-enhancing and survivability-enhancing biostimulants. *Front. Plant. Sci.* **10** (905), 1–14. https://doi.org/10.3389/fpls.2019.00905 (2019).
12. Parisi, M., Alioto, D. & Tripodi, P. Over of the biotic stresses in pepper (*Capsicum* spp): Sources of genetic resistance, molecular breeding and genomics. *International Journal of Molecular Sciences* **21**(7), 2587. https://doi.org/10.3390/ijms21072587 (2020).
13. Thakur, P. et al. Agricultural produce supply chain network of *Capsicum*: Empirical evidence from India. *Economies* **12**(1), 24. https://doi.org/10.3390/economies12010024 (2024).
14. Olutumise, A. I. Determinants of market participation and preference for production of pepper (*Capsicum* spp) among farmers in southwest, Nigeria. *Heliyon* **8**(9), e10585. https://doi.org/10.1016/j.heliyon.2022.e10585 (2022).
15. Pieruschka, R. & Schurr, U. Plant phenotyping: past, present and future. *Plant Phenomics* **2019**, 1–6. https://doi.org/10.34133/2019/7507131 (2019).
16. Helparin, O., Gebremedian, A., Wallach, R. & Moshelion, M. High-throughput physiological phenotyping and screening for the characterization of plant-environment interactions. *Plant J.* **89**, 839–850. https://doi.org/10.1111/tpj.13425 (2017).
17. Walter, A., Liebisch, F. & Hund, A. Plant phenotyping: from bean weighing to image analysis. *Plant. Methods*. **11** (14), 2–11. https://doi.org/10.1186/s13007-015-0056-8 (2015).
18. Costa, C., Schurr, U., Loreto, F., Manesatti, P. & Carpentier, S. Plant phenotyping research trends, a science mapping approach. *Frontiers of Plant Science* **9**(1933), 1–11. https://doi.org/10.3389/fpls.2018.01933 (2019).
19. Fiorani, F. & Schurr, U. Future scenarios for plant phenotyping. *Annual Rev. Plant. Biology*. **64**, 267–291. https://doi.org/10.1146/annurev-arplant-050312-120137 (2013).
20. Fonteijn, H. et al. Automated phenotyping of tomatoes in production greenhouses using robotics and computer vision: From theory to practice. *Agronomy* **11**(8), 1599. https://doi.org/10.3390/agronomy11081599 (2021).
21. Baek, J. et al. High throughput phenotyping for various traits on soybean seeds using image analysis. *Sensors* **20** (248), 1–9. https://doi.org/10.3390/s20010248 (2019).
22. Mansoor, S., Karunathilake, E. M., Tuan, T. T. & Chung, Y. S. Genomics, phenomics, and machine learning in transforming plant research: Advancements and challenges. *Hortic. Plant. J.* **11**(2), 486–503 (2025).
23. Abade, A. S., Ferreira, P. A. & Vidal, F. Plant diseases recognition on images using convolutional neural networks: A systematic review. *Comput. Electron. Agric.* **185**, 106125. https://doi.org/10.1016/j.compag.2021.106125 (2021).
24. Park, E. et al. Phenotyping of low-temperature stressed pepper seedlings using infrared thermography. *J. Biosyst. Eng.* **42**(3), 163–169. https://doi.org/10.5307/JBE.2017.42.3.163 (2017).
25. Johansen, K. et al. Predicting biomass and yield in a tomato phenotyping experiment using UAV imagery and machine learning. *Front. Artif. Intell.* **3** (28), 1–12. https://doi.org/10.3389/frai.2020.00028 (2020).
26. Brewer, M. T., Moyseenko, J. B., Monforte, A. J. & van der Knaap, E. Morphological variation in tomato: a comprehensive study of quantitative trait loci controlling fruit shape and development. *Journal of Experimental Botany* **58**(6), 1339–1349. https://doi.org/10.1093/jxb/erl301 (2007).
27. Rodriguez, G. R. et al. Tomato analyzer: A useful software application to collect accurate and detailed morphological and colorimetric data from two-dimensional objects. *J. Vis. Exp.* **37**(37), 1856. https://doi.org/10.3791/1856 (2010).
28. Weight, C., Parnham, D. & Waites, R. TECHNICAL advance: LeafAnalyser: A computational method for rapid and large-scale analyses of leaf shape variation. *Plant J.* **53**(3), 578–586. https://doi.org/10.1111/j.1365-313X.2007.03330.x (2008).
29. Bylesjo, M. et al. LAMINA: A tool for rapid quantification of leaf size and shape parameters. *BMC Plant Biol.* **8**(1), 82. https://doi.org/10.1186/1471-2229-8-82 (2008).
30. Tanabata, T., Shibaya, T., Hori, K., Ebana, K. & Yano, M. Smartgrain: High-throughput phenotyping software for measuring seed shape through image analysis. *Plant Physiol.* **160**(4), 1871–1880. https://doi.org/10.1104/pp.112.205120 (2012).
31. Hemming, J. et al. A robot for harvesting sweet pepper in greenhouses. Lausanne, Switzerland: Proceedings of the International Conference of Agricultural Engineering (2014).
32. Bac, C. W. et al. Performance evaluation of a harvesting robot of sweet pepper. *J. Field Robotics* **34**, 1123–1139. https://doi.org/10.1002/rob.21709 (2017).
33. Park, J. E. et al. Cost effective image-based phenotyping in Capsicum annuum germplasm for rapid assessment of traits. *Plant. Biotechnol. Rep.* **6**, 1–6 (2025).
34. Naegele, R. P., Mitchell, J. & Hausbeck, M. K. Genetic diversity population structure and heritability of fruit traits and Capsicum annuum. *PlosOne* **11**, e0156969. https://doi.org/10.1371/journal.pone.0156969 (2016).

35. Hill, T. A., Chunthawodtiporn, J., Afshrafi, H., Stoffel, K. & van Deynze, A. Region underlying population structure and the genomics of organ size determination in *Capsicum annuum*. *Plant Genome* **10**(3), 29293816. https://doi.org/10.3835/plantgenome2017.03.0026 (2017).
36. Kior, A., Yudina, L., Zolin, Y., Sukhov, V. & Suhova, E. RGB imaging as a tool for remote sensing of characteristics of terrestrial plants: a review. *Plants* **13** (1262), 1–32. https://doi.org/10.3390/plants13091262 (2024).
37. Mahlein, A.-K. Plant disease detection by imaging sensors – parallels and specific demands for precision agriculture and plant phenotyping. *Plant Disease* https://doi.org/10.1094/PDIS-03-15-0340-FE (2016).
38. Jensen, J. R. *Remote sensing of the environment: an earth resources perspective* 2nd edn. (Pearson Prentice Hall, 2007).
39. Velumani, R. et al. Estimates of maize plant density from UAV RGB images using faster-RCNN detection model: impact of the spatial resolution. *Plant Phenomics* **2021**, 9824843. https://doi.org/10.34133/2021/9824843 (2021).
40. Gene-Mola, J. et al. Assessing the performance of RGB-D sensors for 3D fruit crop canopy characterization under different operating and lighting conditions. *Sensors* **20**(24), 7072. https://doi.org/10.3390/s20247072 (2020).
41. Hennessy, P. J. et al. Evaluation of cameras and image distance for CNN-based weed detection in wild blueberry. *Smart Agricultural Technology* **2**, 100030. https://doi.org/10.1016/j.atech.2021.100030 (2022).
42. Lu, X. et al. Reconstruction method and optimum range of camera-shooting angle for 3D plant modelling using a multi-camera photography system. *Plant Methods* **16**, 1–16. https://doi.org/10.1186/s13007-020-00658-6 (2020).
43. Elsayed, S. et al. Combining thermal and RGB imaging indices with multivariate and data-driven modeling to estimate the growth, water status, and yield of potato under different drip irrigation regimes. *Remote Sensing* **13**(9), 1679. https://doi.org/10.3390/rs13091679 (2021).
44. Wu, Z. et al. Non-contact leaf wetness measurement with laser-induced light reflection and RGB imaging. *Biosyst. Eng.* **244**, 42–52. https://doi.org/10.1016/j.biosystemseng.2024.05.019 (2024).
45. Kasmi, W., Foix, S., Alenya, G. & Andersen, H. J. Indoor and outdoor depth imaging of leaves with time-of-light and stereo vision sensors: Analysis and comparisons. *ISPRS J. Photogramm. Remote Sens.* **88**, 128–146. https://doi.org/10.1016/j.isprsjprs.2013.11.012 (2014).
46. Xia, C., Wang, L., Chung, B-K. & Lee, J-M. In situ 3D segmentation of individual plant leaves using RGB-D camera for agricultural automation. *Sensors* **15** (8), 20463–20479. https://doi.org/10.3390/s150820463 (2015).
47. Brazakis, K. N. et al. Description of olive morphological parameters by using open-access software. *Plant Methods* **13**, 1–15. https://doi.org/10.1186/s13007-017-0261-8 (2017).
48. R Core Team. R: A language and environment for statistical computing. R Foundation for Statistical Computing, Vienna, Austria. URL (2024). https://www.R-project.org/. (2024).
49. de Mendiburu, F. & Agricolae Statistical Procedures for Agricultural Research_. R package version 1.3-7, (2023). https://CRAN.R-project.org/package=agricolae
50. Igathinathane, C., Pordesimo, L. O., Columbus, E. P., Batchelor, W. D. & Methuku, S. R. Shape identification and particles size distribution from basic shape parameters using ImageJ. *Computer and Electronics in Agriculture* **63**(2), 168–182. https://doi.org/10.1016/j.compag.2008.02.007 (2008).
51. Polder, G., Blokker, G. & van der Heijden, G. An ImageJ plugin for plant variety testing. The Netherlands: Biometrics, Wageningen UR. Accessed on 16/11/2024 from (2012). https://edepot.wur.nl/244612
52. Heady, H. F. The measurement and value of plant height in the study of herbaceous vegetation. *Ecology* **38**, 313–320. https://doi.org/10.2307/1931691 (1957).
53. Westoby, M., Falster, D. S., Moles, A. T., Vesk, P. A. & Wright, I. J. Plant ecological strategies: Some leading dimensions of variation between species. *Annu. Rev. Ecol. Evol. Syst.* **33**, 125–159. https://doi.org/10.1146/annurev.ecolsys.33.010802.150452 (2002).
54. Bitella, G. et al. Monitoring plant height and spatial distribution of biometrics with a low-cost proximal platform. *Plants* **13**(8), 1085. https://doi.org/10.3390/plants13081085 (2024).
55. Treder, W., Klamkowski, z, Tryngiel-Gac, A. & Wojcik, K. Application of ImageJ software in the assessment of flowering intensity and growth vigor of pear trees. *J. Hortic. Res.* **29**(2), 85–94. https://doi.org/10.2478/johr-2021-0017 (2021).
56. Polder, G., hovens, H. L. E. & Zweers, A. J. Measuring shoot length of submerged aquatic plants using graph analysis. Proceedings of the ImageJ User and Developer Conference 2010. Mondorf-les-Bains, Luxenbourg, October 27–29, pp 172–177. (2010).
57. Bruness, A. P., de Souza, A. A., Dias, L. W., Villela, F. A. & Aumonde, T. Z. Seedling length in wheat determined by image processing using mathematical tools. *Revista Ciencia Agronomica* **47**(2), 374–379. https://doi.org/10.5935/1806-6690.20160044 (2016).
58. Mack, L. et al. Nondestructive leaf area estimation for chia. *Agron. J.* **109**(5), 1960–1969. https://doi.org/10.2134/agronj2017.03.0149 (2017).
59. Bréda, N. J. Ground-based measurements of leaf area index: A review of methods, instruments, and current controversies. *J. Exp. Bot.* **54**(392), 2403–2417. https://doi.org/10.1093/jxb/erg263 (2003).
60. McDonald, S., Buck, J. & Zenglu, L. Automated, image-based disease measurement for phenotyping resistance to soybean frogeye leaf spot. *Plant Methods* **18**, 1–11. https://doi.org/10.1186/s13007-022-00934-7 (2022).
61. Martin-Gomez, J. J., Saadaoui, E. & Cervantes, E. Seed shape of Castor Bean (*Ricinus communis* L.) grown in different regions of Tunisia. *J. Agric. Ecol. Res. Int.* **8**(1), 1–11. https://doi.org/10.9734/JAERI/2016/23934 (2016).
62. Felix, C. F., Kratz, D., Ribeiro, R. & Nogueira, A. C. Characterization and differentiation of forest species by seed image analysis: A new methodological approach. *Ciênc. Florestal* **33**(3), e73427. https://doi.org/10.5902/1980509873427 (2023).
63. Arredondo-Valdez, J. et al. Characterization of mature cladodes of *Opuntia ficus-indica* L. using morphological and colorimetric descriptors. *J. Exp. Biol. Agric. Sci.* **10**(2), 335–343. https://doi.org/10.18006/2022.10(2).335.343 (2022).
64. Cevantis, E., Martin, J. J. & Saadaoui, E. Updated methods for seed shape analysis. *Scientifica* **4**, 1–10. https://doi.org/10.1155/2016/5691825 (2016).
65. Marcel, H., Javier, M.-G., Emilio, C., Roman, H. & Luis, R. L. Seed shape and size of *Silene latifolia*, differences between sexes, and influence of the parental genome in hybrids with *Silene dioica*. *Front. Plant Sci.* **15**, 1297676. https://doi.org/10.3389/fpls.2024.1297676 (2024).
66. Martin-Gomez, J. J. et al. The outline of seed silhouettes: A morphological approach to *Silene* (Caryophyllaceae). *Plants* **11**(23), 3383. https://doi.org/10.3390/plants11233383 (2022).
67. Sharma, R., Kumar, M. & Alam, M. S. Image processing techniques to estimate weight and morphological parameters for selected wheat refractions. *Sci. Rep.* **11**(1), 20953. https://doi.org/10.1038/s41598-021-00081-4 (2021).
68. Sheikh, M. et al. Integrating artificial intelligence and high-throughput phenotyping for crop improvement. *J. Integr. Agric.* **23** (6), 1787–1802 (2024).
69. Ubbens, J., Stavness, I., Pound, M. P. & Guo, W. Deep learning in plant phenotyping: The first ten years. *Plant Phenomics* **7**(4), 10062. https://doi.org/10.1016/j.plaphe.2025.100062 (2025).
70. Meraj, T. et al. Computer vision-based plants phenotyping: A comprehensive survey. *iScience* **27**(1), 108709. https://doi.org/10.1016/j.isci.2023.108709 (2023).
71. Lobet, G. Image analysis in plant sciences: publish then perish. *Trends in Plant Science* **22**(7), 559–566. https://doi.org/10.1016/j.tplants.2017.05.002 (2017).
72. Philips, R. L. Mobilizing science to break yield barriers. *Crop Science* **50**, S-99-S−108. https://doi.org/10.2135/cropsci2009.09.0525 (2010).
73. Karunathilake, E. M., Le, A. T., Heo, S., Chung, Y. S. & Mansoor, S. The path to smart farming: Innovations and opportunities in precision agriculture. *Agriculture* **13** (8), 1593 (2023).

74. Joosen, R. V. L. et al. Visualizing the genetic landscape of arabidopsis seed performance. *Plant Physiol.* **158**, 570–589. https://doi.org/10.1104/pp.111.186676 (2012).
75. Golzarain, M. R. et al. Accurate inference of shoot biomass from high-throughput images of cereal plants. *Plant Methods* **7**, 1–11. https://doi.org/10.1186/1746-4811-7-2 (2011).

Acknowledgements
We acknowledge the Rural Development Administration (RDA), the National Agricultural Sciences (NAS), the Plant Phenomics Centre, the Korea - Africa Food and Agriculture Cooperation Initiative (KAFACI), and CSIR – Plant Genetic Resources Research Institute for their diverse contributions to this research. We also thank Ms. Seong Mi Hong, Mr. Jae Young Kim, Dr. Dong Su Jung, and Ms. Su Jong Ra for their technical assistance.

Author contributions
E.O.M., J.S., J.S., H.O., H.O., and S.M: Writing - review & editing, Writing-original draft, Visualization, Validation, Methodology, Investigation, Data curation. J.B., S.L.K., S.L.K., A.M.A., A.M.A., and S.M: Writing - review & editing, Project administration, Supervision, Funding acquisition, Conceptualization. J.S., J.B., J.B., A.M.A., A.M.A and Y.S.C: Visualization, Investigation, Data curation. E.O.M, H.O, A.M.A and J.B: Writing - review & editing, Validation.

Funding
This research was supported by the Cooperative Research Program for Agriculture Science and Technology Development (Project No. PJ01723801), and the Korea-Africa Food and Agriculture Cooperation Initiative (KAFACI Young Scientist Project-2024), Rural Development Administration (RDA), the Republic of Korea.

Declarations

Competing interests
The authors declare no competing interests.

Additional information
Supplementary Information The online version contains supplementary material available at https://doi.org/10.1038/s41598-026-46601-y.

Correspondence and requests for materials should be addressed to J.B. or S.M.

Reprints and permissions information is available at www.nature.com/reprints.

Publisher's note Springer Nature remains neutral with regard to jurisdictional claims in published maps and institutional affiliations.

Open Access This article is licensed under a Creative Commons Attribution-NonCommercial-NoDerivatives 4.0 International License, which permits any non-commercial use, sharing, distribution and reproduction in any medium or format, as long as you give appropriate credit to the original author(s) and the source, provide a link to the Creative Commons licence, and indicate if you modified the licensed material. You do not have permission under this licence to share adapted material derived from this article or parts of it. The images or other third party material in this article are included in the article's Creative Commons licence, unless indicated otherwise in a credit line to the material. If material is not included in the article's Creative Commons licence and your intended use is not permitted by statutory regulation or exceeds the permitted use, you will need to obtain permission directly from the copyright holder. To view a copy of this licence, visit http://creativecommons.org/licenses/by-nc-nd/4.0/.

© The Author(s) 2026